Electronic Supplementary Information

Creating a blue-light excitable, ultra-broadband and relatively long-wavelength near-infrared emission in Cr^{3+}-activated garnet via controlling cationic disorder

Chaojie Li[a], and Jiyou Zhong[a,b,*]

[a]School of Physics and Optoelectronic Engineering, Guangdong University of Technology, Guangzhou 510006, China. E-mail: jyzhong2016@gdut.edu.cn.

[b]Guangdong Provincial Key Laboratory of Sensing Physics and System Integration Applications, Guangdong University of Technology, Guangzhou 510006, China.

Experimental Section

S1. Synthesis **：** Garnets with formula of $Na_xCa_{3-2x}Gd_xIn_{2-y}Cr_yGe_3O_{12}$ (x = 0, 0.3, 0.6, 0.9, 1.2, and 1.5; y = 0, and 0.06) were synthesized by high-temperature solid-state reaction. Firstly, $NaHCO_3$ (Aladdin, 99.5%), $CaCO_3$ (Aladdin, 99.5%), Gd_2O_3 (Macklin, 99.99%), In_2O_3 (Aladdin, 99.99%), GeO_2 (Aladdin, 99.99%), and Cr_2O_3 (Aladdin, 99.99%) were used as the raw materials and weighed according to the stoichiometric ratio. In addition, an excess of 5 wt% $NaHCO_3$ were added to compensate for the loss of Na^+ at high temperature and 5 wt% CaF_2, NaF, and NH_4F were also added as flux, respectively. Secondly, the weighed raw materials were thoroughly ground in an agate mortar with a pestle for 30 minutes. Then, the mixtures were transferred to a corundum crucible and sent to a tube furnace for sintering. The sintering process was set to heat at 1350 ℃ for 8 hours in air, with a heating and cooling rate of 3 ℃/min. Finally, after cooling to room temperature, the products were thoroughly ground to a fine powder for subsequent measurements.

S2. Characterization **：** The phase purity of samples was confirmed using powder X-ray diffraction obtained by the X'Pert^3 PANalytical diffractometer (Cu Kα, λ = 1.5406 Å). Rietveld refinements of the diffractograms was performed using the General Structure Analysis System (GSAS) software and EXPGUI interface with a shifted Chebyshev function employed to describe the background.[1] The crystal structure was analyzed and visualized by VESTA.[2] Raman spectra were measured using a solid-state laser excitation (532 nm) on InVia Raman Microscope (Renishaw, England). A UV-vis-NIR spectrophotometer (UV-3600 Plus, Shimadzu, Japan) was used to measure the diffuse reflectance (DR) spectra of these garnet samples. The room-temperature photoluminescence excitation (PLE), photoluminescence emission (PL), and decay curves of the as-prepared samples were measured using the FLS-1000 fluorescence spectrophotometer (Edinburgh Instruments), which equipped with a Xenon flash lamp (450 W, Osram) as the excitation source and a liquid-nitrogen cooled NIR photomultiplier tube as a detector (Hamamatsu, R5509, InP/InGaAsP). The internal quantum efficiency (IQE) and absorption efficiency (AE) were determined on a Quantaurus-QY Plus C13534-11 (Hamamatsu Photonics) based on the integrating sphere with spectralon as a reference. The prototype NIR

pc-LED was fabricated by coating the mixture of $Na_xCa_{3-2x}Gd_xIn_{1.94}Ge_3O_{12}$:0.06$Cr^{3+}$ (x = 0, 0.6, and 1.5) phosphors and resin in a ratio of 1:1 (in weight) onto a 455 nm LED chip. The NIR photoelectric properties of the as-prepared pc-LED device were recorded using a HAAS2000 photoelectric measurement system (EVERFINE, China).

Supplementary Equations

The crystal field strength parameter (Dq/B) estimated by the following equations:[3,4]

$$10Dq = E(^4A_2 \rightarrow {}^4T_2) - \Delta S/2 \quad \textbf{(Eqn. S1)}$$

$$Dq/B = \frac{15(m-8)}{m^2 - 10m} \quad \textbf{(Eqn. S2)}$$

$$m = \frac{E(^4A_2 \rightarrow {}^4T_1) - E(^4A_2 \rightarrow {}^4T_2)}{Dq} \quad \textbf{(Eqn. S3)}$$

where Dq and B represents crystal field splitting energy and the Racah parameter, respectively; while $E(^4A_2 \rightarrow {}^4T_1)$ and $E(^4A_2 \rightarrow {}^4T_2)$ correspond to the peak positions of the excitation bands of the $^4T_1$ and $^4T_2$ levels.

The curves can be well fitted by a single-exponential function:[5]

$$I_t = I_0 \exp(-\frac{t}{\tau}) \quad \textbf{(Eqn. S4)}$$

where I_t represents the emission intensity at time t, I_0 is the initial intensity at t = 0, and τ is the calculated lifetime.

Supplementary Figures and Tables

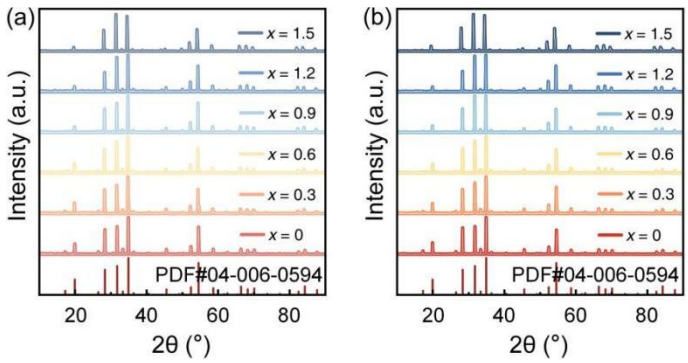

Fig. S1. (a-b) XRD patterns of the $Na_xCa_{3-2x}Gd_xIn_{2-y}Ge_3O_{12}$:$yCr^{3+}$ (x = 0-1.5; y = 0 and 0.06) samples compared with the standard XRD pattern.

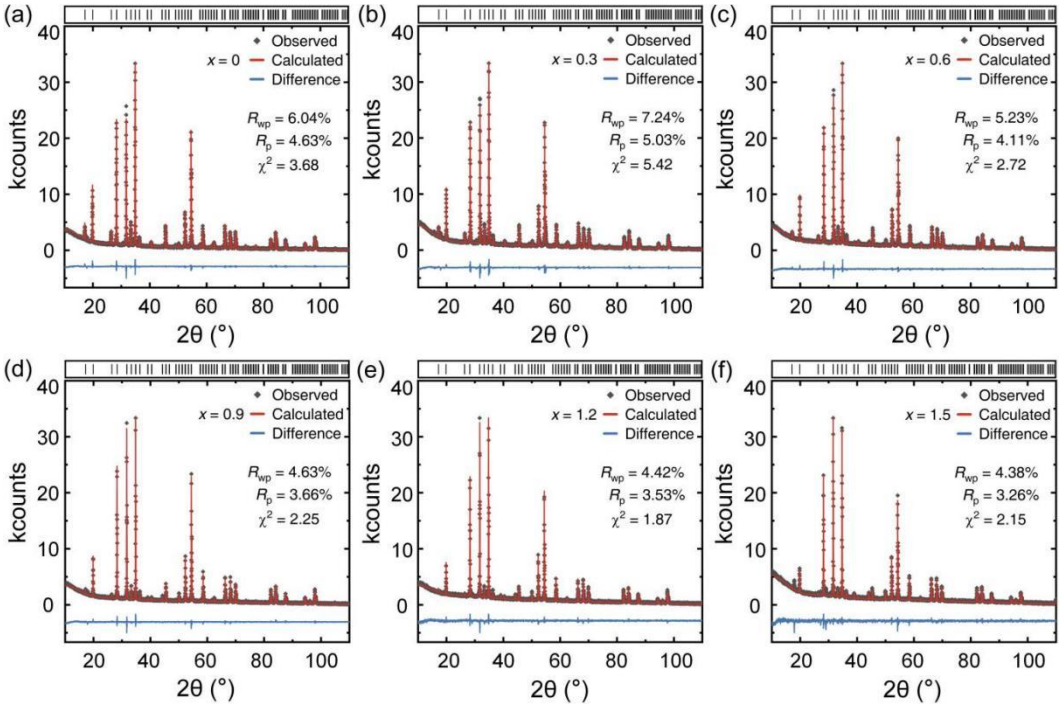

Fig. S2. (a-f) Rietveld refinement of XRD pattern for $Na_xCa_{3-2x}Gd_xIn_{1.94}Ge_3O_{12}$:$0.06Cr^{3+}$ (x = 0-1.5) samples.

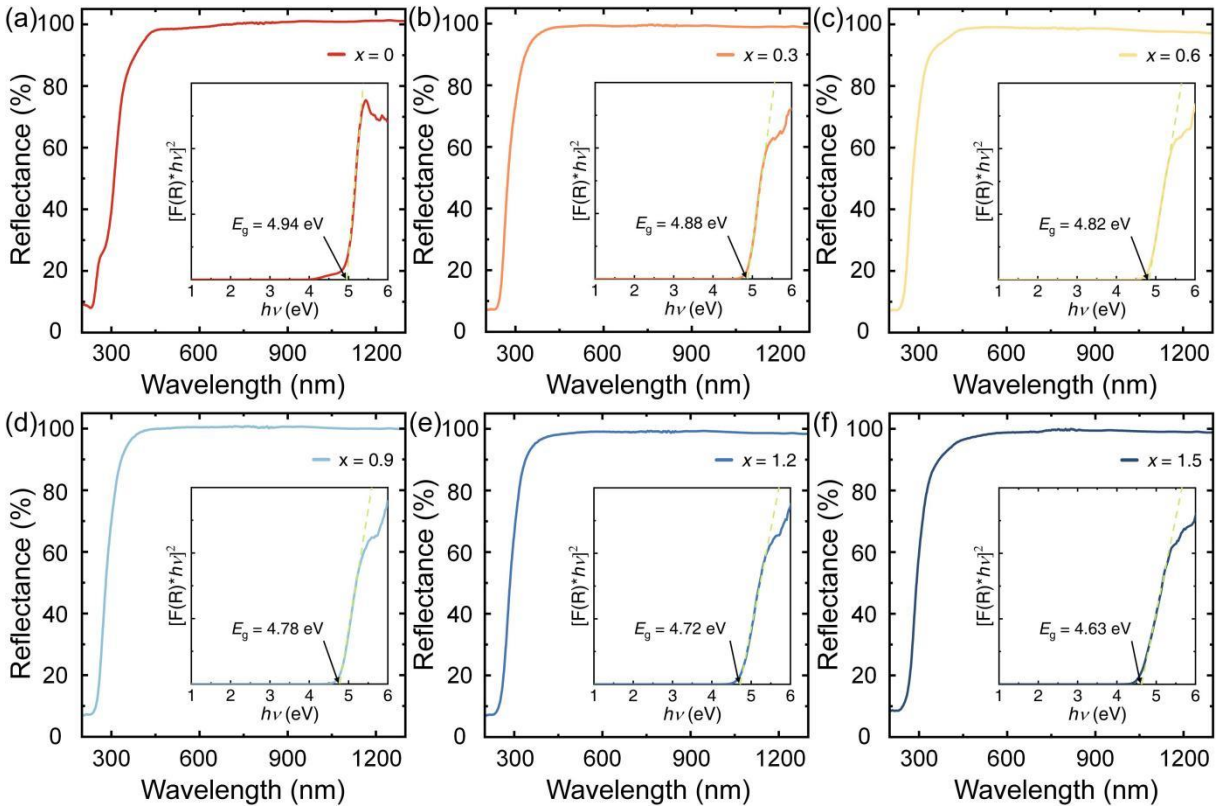

Fig. S3. (a-f) Diffraction reflection (DR) spectra and optical band gap (inset) of $Na_xCa_{3-2x}Gd_xIn_{1.94}Ge_3O_{12}$:$0.06Cr^{3+}$ (x = 0-1.5) samples.

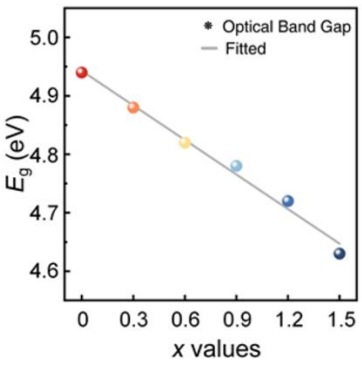

Fig. S4. Linearly fitting the optical band gap of $Na_xCa_{3-2x}Gd_xIn_{1.94}Ge_3O_{12}$:0.06$Cr^{3+}$ (x = 0-1.5) as function of x.

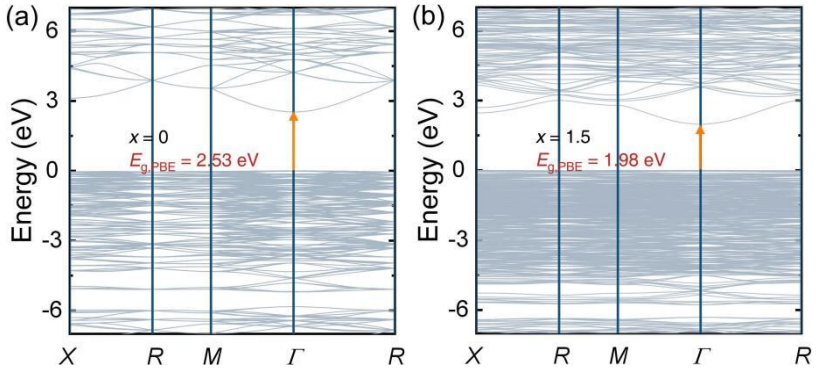

Fig. S5. (a-b) The band structures of $Na_xCa_{3-2x}Gd_xIn_2Ge_3O_{12}$ (x = 0 and 1.5) hosts.

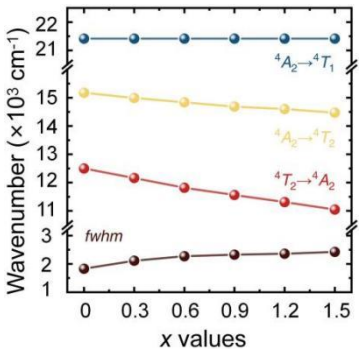

Fig. S6. Excitation and emission energy, and *fwhm* as a function of x value.

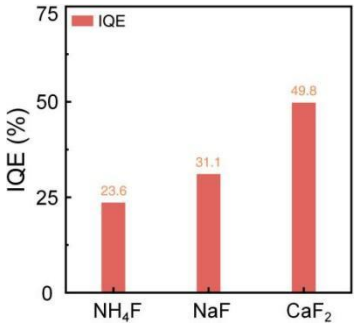

Fig. S7. IQE, AE, and EQE of $Na_{1.5}Gd_{1.5}In_2Ge_3O_{12}$:$Cr^{3+}$ by optimized sintering using different fluxes.

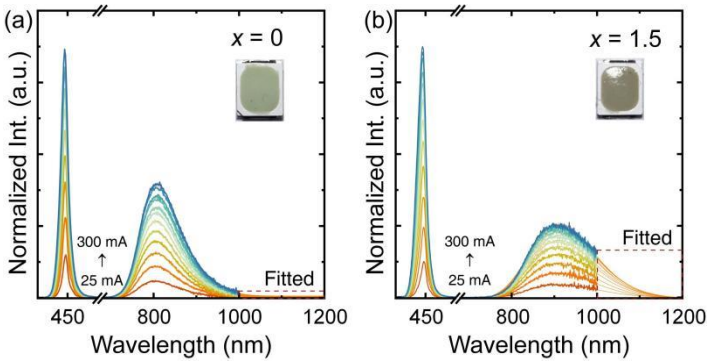

Fig. S8. (a-b) Electroluminescence spectra of NIR pc-LED devices (inset) fabricated by using $Na_xCa_{3-2x}Gd_xIn_{1.94}Ge_3O_{12}$:0.06$Cr^{3+}$ (x = 0 and 1.5) samples.

Table S1 Refined results of $Na_xCa_{3-2x}Gd_xIn_{1.94}Ge_3O_{12}$:0.06$Cr^{3+}$ (x = 0, 0.6, and 1.5) Samples.

x values	x = 0	x = 0.6	x = 1.5
Radiation type; λ (Å)	X-ray; 1.5406	X-ray; 1.5406	X-ray; 1.5406
2θ (degree)	10 - 120	10 - 120	10 - 120
Temperature (K)	298	298	298
Space group	$Ia\bar{3}d$	$Ia\bar{3}d$	$Ia\bar{3}d$
$\alpha = \beta = \gamma$ (degree)	90.00	90.00	90.00
$a = b = c$ (Å)	12.56453(7)	12.58451(9)	12.61052(6)
V (Å^3)	1983.53(3)	1993.01(2)	2005.39(4)
Profile R-factor, R_p (%)	0.0463	0.0411	0.0326
Weighted profile R-factor, R_{wp} (%)	0.0604	0.0523	0.0438
χ^2	3.68	2.72	2.15

Table S2. Refined atomic position of $Na_xCa_{3-2x}Gd_xIn_{1.94}Ge_3O_{12}$:0.06$Cr^{3+}$ (x = 0, 0.6, and 1.5) Samples.

x values	Atom	Wyck. position	Occupation	x	y	z
	Ca	24*c*	1	0.12500(0)	0	0.25000(0)
	In	16*a*	0.97	0	0	0
x = 0	Ge	24*d*	1	0.37500(0)	0	0.25000(0)
	O	96*h*	1	0.08685(6)	0.19167(2)	0.28295(7)
	Cr	16*a*	0.03	0	0	0
	Na	24*c*	0.2	0.12500(0)	0	0.25000(0)
	Ca	24*c*	0.8	0.12500(0)	0	0.25000(0)
	Gd	24*c*	0.2	0.12500(0)	0	0.25000(0)
x = 0.6	In	16*a*	0.97	0	0	0
	Ge	24*d*	1	0.37500(0)	0	0.25000(0)
	O	96*h*	1	0.09034(3)	0.19106(3)	0.28588(3)
	Cr	16*a*	0.03	0	0	0
	Na	24*c*	0.5	0.12500(0)	0	0.25000(0)
	Gd	24*c*	0.5	0.12500(0)	0	0.25000(0)
x = 1.5	In	16*a*	0.97	0	0	0
	Ge	24*d*	1	0.37500(0)	0	0.25000(0)
	O	96*h*	1	0.08795(2)	0.19541(1)	0.28399(0)

	Cr	16*a*	0.03	0	0	0

Table S3. Local coordination of octahedral site in $Na_xCa_{3-2x}Gd_xIn_{1.94}Cr_{0.06}Ge_3O_{12}$ (x = 0, 0.6, and 1.5).

x values	Bonds	Bond length (Å)	O-In-O bond angle (°)	Distortion index	*σ*
x = 0	In-O	2.207(3)	86.131(3) 86.131(3)	0	4.04
		2.207(3)	93.871(3) 93.871(3)		
		2.207(3)	86.131(3) 93.871(3)		
		2.207(3)	93.871(3) 93.871(3)		
		2.207(3)	93.871(3) 86.131(3)		
		2.207(3)	86.131(3) 86.131(3)		
x = 0.6	In-O	2.189(4)	87.031(6) 87.031(6)	0	3.10
		2.189(4)	92.971(6)		
		2.189(4)	92.971(6)		
		2.189(4)	87.031(6)		
		2.189(4)	92.971(6)		
		2.189(4)	92.971(6)		
		2.189(4)	92.971(6)		
		2.189(4)	92.971(6)		
		2.189(4)	87.031(6)		
		2.189(4)	87.031(6) 87.031(6)		
x = 1.5	In-O	2.175(5)	87.282(4) 87.282(4)	0	2.84
		2.175(5)	92.722(4) 92.722(4)		
		2.175(5)	87.282(4) 92.722(4)		
		2.175(5)	92.722(4) 92.722(4)		
		2.175(5)	92.722(4) 87.282(4)		
		2.175(5)	87.282(4) 87.282(4)		

Table S4. The Crystal Field Parameters and of $Na_xCa_{3-2x}Gd_xIn_{1.94}Ge_3O_{12}$:0.06$Cr^{3+}$ (x = 0 - 1.5) Samples.

x values	E($^4T_1$) (cm^{-1})	E($^4T_2$) (cm^{-1})	E($^4T_2 \rightarrow {}^4A_2$) (cm^{-1})	*Dq* (cm^{-1})	*B* (cm^{-1})	*Dq*/*B*
0	21413	15175	12500	1384	654	2.12
0.3	21413	14993	12165	1358	690	1.97
0.6	21413	14837	11820	1333	724	1.84
0.9	21413	14684	11561	1312	761	1.72
1.2	21413	14599	11312	1296	786	1.65
1.5	21413	14472	11050	1276	824	1.55

Supplementary References

1 B. H. Toby and R. B. Von Dreele, *J. Appl. Crystallogr.*, 2013, **46**, 544–549.
2 K. Momma and F. Izumi, *J. Appl. Crystallogr.*, 2011, **44**, 1272–1276.
3 Y. Tanabe and S. Sugano, *J. Phy. Soc. Japan*, 1954, **9**, 766–779.
4 X. Zhou, W. Geng, J. Li, Y. Wang, J. Ding and Y. Wang, *Adv. Opt. Mater.*, 2020, **8**, 1–8.
5 Z. Xia and R. Liu, *J. Phy. Chem. C*, 2012, **116**, 15604–15609.